(Article begins on next page)

28/04/2024 10:55

The first Italian blast-induced liquefaction test (Mirabello, Emilia-Romagna, Italy): description of the experiment and preliminary results

AMOROSO SARA[1]*, MILANA GIULIANO[2], ROLLINS KYLE M.[3], COMINA CESARE[4], MINARELLI LUCA[5], MANUEL MARIA R.[6], MONACO PAOLA[7], FRANCESCHINI MARCO[8], ANZIDEI MARCO[2], LUSVARDI CAMERON[3], CANTORE LUCIANA[1], CARPENA ANDREA[9], CASADEI STEFANO[10], CINTI FRANCESCA R.[2], CIVICO RICCARDO[2], COX BRADY R.[11], DE MARTINI PAOLO MARCO[2], DI GIULIO GIUSEPPE[1], DI NACCIO DEBORAH[1], DI STEFANO GIUSEPPE[2], FACCIORUSSO JOHANN[12], FAMIANI DANIELA[2], FIORELLI FEDERICO[8], FONTANA DANIELA[13], FOTI SEBASTIANO[14], MADIAI CLAUDIA[12], MARANGONI VALERIA[4], MARCHETTI DIEGO[15], MARCHETTI SILVANO L.[15], MARTELLI LUCA[16], MARIOTTI MAURO[17],MUSCOLINO ELENA[8], PANCALDI DAVIDE[8], PANTOSTI DANIELA[2], PASSERI FEDERICO[14], PESCI ARIANNA[18], ROMEO GIOVANNI[2], SAPIA VINCENZO[2], SMEDILE ALESSANDRA[2], STEFANI MARCO[19], TARABUSI GABRIELE[18], TEZA GIORDANO[20], VASSALLO MAURIZIO[1], VILLANI FABIO[1]

[1]Istituto Nazionale di Geofisica e Vulcanologia, L'Aquila, Italy.

[2]Istituto Nazionale di Geofisica e Vulcanologia, Rome, Italy.

[3]Brigham Young University, Provo, Utah, USA.

[4]University of Turin, Turin, Italy.

[5]Geotema srl, University of Ferrara spin-off company, Ferrara, Italy.

[6]GEO Geotecnica e Geognostica srl, Arpino, Italy.

[7]University of L'Aquila, L'Aquila, Italy.

[8]Teleios srl, Castel Maggiore, Italy.

[9]Georeflex srl, Piacenza, Italy.

[10]INDGEO due srl fondazioni speciali, San Giuseppe di Comacchio, Italy.

[11]The University of Texas at Austin, Austin, Texas, USA.

[12]University of Florence, Florence, Italy.

[13]University of Modena and Reggio Emilia, Modena, Italy.

[14]Politecnico di Torino, Turin, Italy.

[15]Studio Prof. Marchetti srl, Rome, Italy.

[16]Emilia-Romagna Region, Bologne, Italy.

[17]Sara Electronic Instruments srl, Perugia, Italy.

[18]Istituto Nazionale di Geofisica e Vulcanologia, Bologne, Italy.

[19]University of Ferrara, Ferrara, Italy.

[20]University of Padua, Padua, Italy.

Abstract

Soil liquefaction can result in significant settlement and reduction of load-bearing capacity. Moreover, the increase and the accumulation of pore pressure during an earthquake and its post-seismic dissipation can generate permanent deformations and settlements. The quantitative evaluation of post-liquefaction settlements is of extreme importance for engineering purposes, i.e. for earthquake-resistant design of new buildings and safety evaluation of existing ones. Quantifying the extent of these phenomena is, however, rather difficult. Uncertainties arise from the stochastic nature of the earthquake loading, from the simplifications of soil models, and from the difficulty in establishing correlations between the pre-earthquake soil state and the post-seismic deformations. Field scale liquefaction tests, under controlled conditions, are therefore important for a correct quantification of these phenomena. Recent experiences (e.g. New Zealand, United States) show that liquefaction can be induced and monitored with field scale blast tests to study the related effects on soil geotechnical properties. Within this framework this paper introduces the preliminary results obtained from a research project on blast-induced liquefaction at the field scale; tests were performed at a trial site located in Mirabello (Ferrara, Italy), a village strongly affected by liquefaction phenomena during the 2012 Emilia Romagna earthquake. Invasive tests, such as piezocone, seismic dilatometer and down-hole tests, and non-invasive tests were carried out before and after the execution of two blast test sequences to study the variation in physical properties of the soils. Pore pressure transducers, settlement profilometers, accelerometers and an instrumented micropile were installed with the objective of measuring, during and after the detonations, the generation and subsequent dissipation of the pore pressure, the vertical deformations, and the blast-induced ground motions respectively. Variations in load distribution on deep foundations due to soil liquefaction were also evaluated on a test micropile instrumented with a strain gauge chain. Topographical surveys were carried out to measure ground surface settlements. Laboratory tests and trenches also provided increase understanding of the site characteristics.

1. Introduction

The occurrence of liquefaction phenomena can result in significant settlement and reduction of load-bearing capacity. In particular, the dissipation of earthquake-induced pore pressure can initiate liquefaction-induced settlements, frequently causing damage to foundations and lifelines [Kramer 1996]. According to the Eurocode 8 [EN 1998-5 2004], the quantitative evaluation of post-liquefaction settlements is of extreme importance for engineering purposes, i.e. for earthquake-resistant design of new buildings and safety evaluation of existing ones. In this respect, different procedures for the deformation assessment were developed using ground response analyses [Pyke et al. 1975], or simplified procedures [Tokimatsu and Seed 1987, Ishihara and Yoshimine 1992]. Most of the currently published methods are based on in situ geotechnical

investigations [Tokimatsu and Seed 1987, Ishihara and Yoshimine 1992, Idriss and Boulanger 2008, Zhang et al. 2002]. Either the standard penetration test or the cone penetration test is used in this respect. Few published papers calculate the liquefaction-induced settlement based on the shear wave velocity [Yi 2010], that can be measured by geophysical surveys or seismic geotechnical in situ tests, such as the seismic dilatometer test. However, quantifying the extent of these phenomena is rather difficult, due to the stochastic nature of the earthquake loading, the simplifications of soil models and the difficulty to have reliable correlations between the actual soil state and the post-seismic deformations [Győri et al. 2011].

For the above reasons, the blast technique has been developed based on the controlled detonation of explosives to generate long duration cyclic shaking of the ground and thereby to test the in situ soil liquefaction potential, as shown by recent experiences in New Zealand and United States [e.g. Wentz et al. 2015, Finno et al. 2016]. By inducing multiple shear strain cycles and observing pore pressure build-up, blast tests cause acceleration at high frequency, much higher than that of real earthquakes, but ground velocity and displacement amplitudes are similar to those generated by a strong earthquake. In situ geotechnical monitoring, laboratory investigations and geophysical surveys are usually coupled with the detonations to optimize their effectiveness [Ashford et al. 2004, Rollins et al. 2004, Gohl et al. 2001] and to evaluate soil parameters variations before and after liquefaction.

The present work shows the activities performed for a blast experiment in a target site in northern Italy. The paper introduces the preliminary results in the framework of a research project on induced liquefaction, performed at a trial site located in Mirabello (Ferrara, Italy), a village strongly affected by liquefaction phenomena during the 2012 Emilia Romagna earthquake [Caputo and Papathanasiou 2012, Emergeo Working Group 2013, Fioravante et al. 2013, Vannucchi et al. 2012, Facciorusso et al. 2016]. At the Mirabello site, an intensive geological, geotechnical and geophysical campaign was carried out before and after the execution of two blast test sequences. Pore pressure transducers and settlement profilometers were installed with the purpose of measuring, during and after the blast test, the generation and subsequent dissipation of the pore water pressure along with the vertical deformations, respectively. Detailed topographical surveys were also performed to monitor vertical deformations of the ground surface.

2. Selection of the test site

The selection of an experimental site where liquefaction effects are well documented was chosen as a reliable criteria to test the technique and to check its results. In this respect the 2012 Emilia sequence (M_L 5.9 and M_L 5.8 on May 20 and 29, 2012, respectively) produced significant and widespread liquefaction effects in various areas of the Emilia-Romagna Region (Figure 1a), as observed during extensive field reconnaissance by INGV-Emergeo [Emergeo Working Group 2013], University of Ferrara [Caputo and Papathanasiou 2012] and Emilia-Romagna Region [Regione Emilia-Romagna 2012]. The most significant and

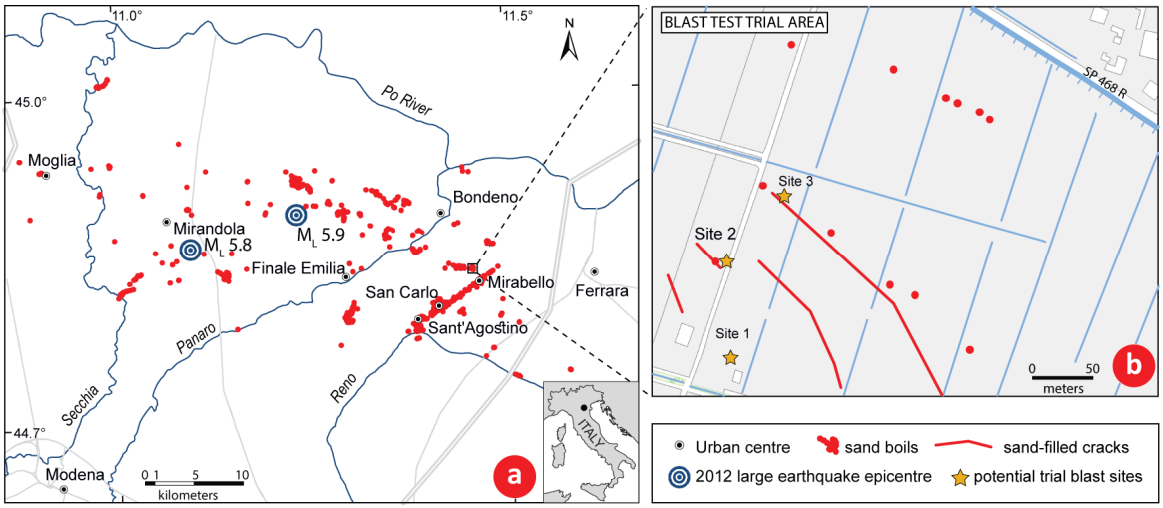

Figure 1. Map of the liquefaction phenomena following 2012 Emilia earthquake (data from Emergeo Working Group [2013], Caputo and Papathanasiou [2012] and Regione Emilia-Romagna [2012]) (a); map of the potential trial blast sites in Mirabello village (b).

widespread liquefaction phenomena occurred in the villages of San Carlo and Mirabello (since 2017 Terre del Reno municipality). Mirabello was therefore chosen to carry out the blast test trial.

The selection of the site was then guided by the necessity to limit the level of vibrations generated by the detonation under an acceptable threshold that is strictly related to the human perception and to the presence of buildings. Following previous blast liquefaction experiences the ground peak particle velocity (*PPV*) is a parameter connected with the human perception. *PPV*, expressed in m/s, can be estimated as:

$$PPV = 1.47\left(\frac{R}{\sqrt{W}}\right)^{-1.325} \quad (1)$$

$$PPV = 3.21\left(\frac{R}{\sqrt{W}}\right)^{-1.325} \quad (2)$$

where R is the distance (m), from the center of a blast area and W is the weight (kg), of the individual charges. Eq. (1) indicates the mean *PPV* and Eq. (2) refers to the upper bound *PPV* according to Kato et al. [2015]. On average *PPV* values < 1.5-3.0 mm/s may be barely perceptible to humans, while PPV values < 3.0-5.0 mm/s prevent historic and residential buildings from damage. Given a charge weight of 4 kg, a safety distance of 350 m would generate a PPV between 1.5 mm/s and 3.0 mm/s which is an acceptable value for human perception and damage to building.

The above considerations made it desirable to locate the blast test site 1.5 km from the center of Mirabello village, where liquefaction phenomena had been detected, but relatively few buildings (sometimes ruins) are present and were at least 350 m from the trial area. Preliminarily, three potential sites were selected in a narrow area (Figure 1b). After the 2012 Emilia seismic

sequence widespread liquefaction phenomena were observed at Site 2 and Site 3, no evidence of sand boils was detected at Site 1. In detail Site 2 was settled on one large 2012 liquefaction evidence, showing as aligned multiple sand volcanos, about 3 to 8 m large and 33-36 m long.

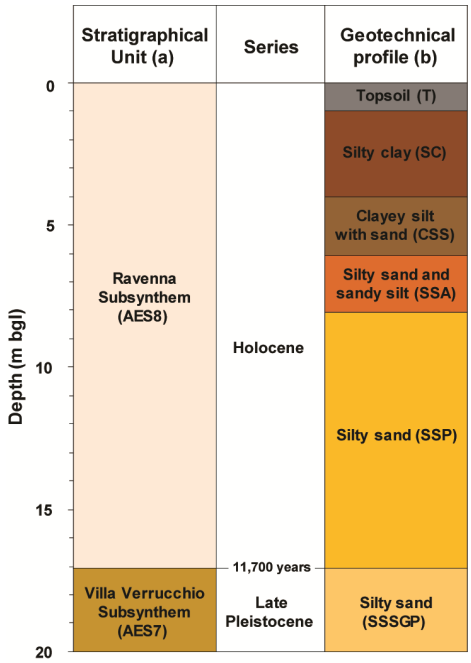

Figure 2. Mirabello trial site: stratigraphical profile (a); simplified geotechnical model (b).

The stratigraphic succession of the selected area consists of Holocene and late Pleistocene sediments, accumulated in alluvial plain environments [Regione Emilia-Romagna 2013], as schematically shown in Figure 2a. The proposed chronostratigraphical scheme (Figure 2a) was obtained using also stratigrapical correlations based on radiocarbon datings [Amorosi et al. 2016, Bruno et al. 2016). Moving downward from the ground surface, units can be schematically described: the surface is usually composed of reworked soils and/or fine sediments that possibly incorporate extruded liquefied sand; then fine-grained sediments, deposited in an interfluvial depression (Ravenna Subsynthem AES8), are encountered; below fluvial coarse-grained sediments of heterogeneous Apenninic provenance, deposited in crevasse splays in pre-Roman times (Ravenna Subsynthem AES8), are located; finally silty sands of the Po River channel (Ravenna Subsynthem AES8) are detected before the Syn-Glacial Po River braided deposits composed of coarse-grained sands (Villa Verrucchio Subsynthem AES7). Details on the abovementioned stratigraphical units can be found in Minarelli et al. [2016].

On January 2016 in each of the three sites 20 m-deep piezocone tests (Site1-CPTu1, Site2-CPTu2, Site3-CPTu3) were performed in order to provide a first-order liquefaction assessment according to the "simplified procedure". The CPT-based liquefaction analyses were carried out using the method proposed by Idriss and Boulanger [2008], assuming the seismic input (moment magnitude M_W = 6.14, peak ground acceleration PGA = 0.2175g) obtained from the seismic microzonation study of the Mirabello municipality [Regione Emilia-Romagna 2013, Geotema 2014]. The ground water table (GWT) was preliminarly assumed equal to the in situ GWT, as provided by the piezocone tests. The estimation of the liquefaction potential index according to Iwasaki et al. [1982] provided low liquefaction risk (almost zero) at Site 1 and from low to high risk at Site 2 and Site 3, confirming the observations from the 2012 earthquake. As a consequence, Site 1 was directly excluded for the blast experiment. The selection of Site 2 was supported by the

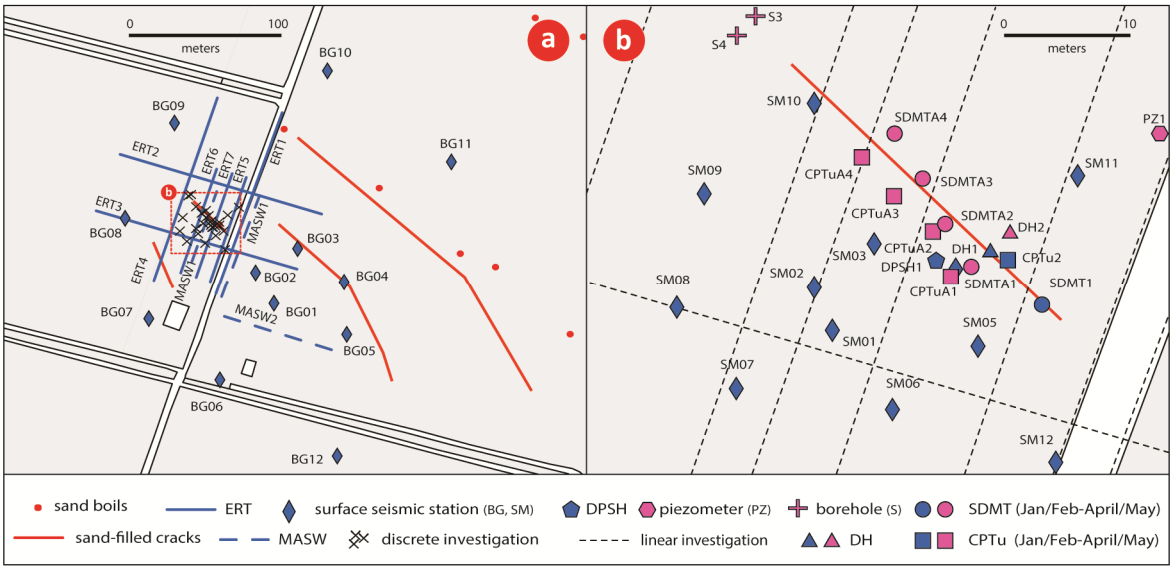

Figure 3. Map of pre-blast investigations at the trial Mirabello blast test site: blue color is related to the January/February site campaign, and pink color indicates the April/May investigations.

greater thickness of the main potential liquefiable layer (i.e. fluvial Apenninic coarse-grained deposits) that corresponds to 2 m (from 6 to 8 m bgl) at Site 2 and to 1 m (from 7 to 8 m bgl) at Site 3.

3. Design of the blast test

3.1. Pre-blast site investigation and liquefaction assessment

Soon after the selection of Site 2, in January and February 2016 a preliminary geological, geotechnical and geophysical characterization was carried out in proximity to the observed liquefaction phenomena. The aim of the surveys was to characterize the subsoil model at Site 2, and consequently to set-up the blast layout (blue symbols and lines in Figures 3a and 3b). Besides the piezocone test (CPTu2), the in situ investigations (Figure 3b) consisted of: one 20 m-deep borehole (S1), four standard penetration tests within S1, one 19 m-deep seismic dilatometer test (SDMT1), and one 15 m-deep dynamic probe super heavy test (DPSH1). The GWT in the borehole was located at 4.2 m bgl, confirming the CPTu evaluation. Nineteen disturbed samples were retrieved with coring and a SPT (Standard Penetration Test) split barrel sampler to perform sieve analyses and Atterberg limits, while five disturbed samples on sandy deposits and one disturbed sample on a peaty layer were retrieved with coring to execute compositional analyses and radiocarbon dating, respectively. Moreover, four undisturbed samples were also retrieved with a Shelby sampler to perform dynamic and cyclic laboratory tests, that are still ongoing. Geophysical tests (Figures 3a, 3b) included: two down-hole tests (DH1) within S1 borehole, one by means of a seismic chain of 8 triaxial (10 Hz) geophones at 1 m spacing, and one with a pair of triaxial geofone (10 Hz), three MASW (Multichannel

Analysis of Suface Waves) using an array of 72 (MASW1, MASW2) or 48 (MASW3), vertical (4.5 Hz) geophones at 1 m spacing, two P-wave and two S-wave tomographies along MASW1 and MASW2 profiles, seven 2D electrical resistivity tomographies via 64 electrodes at 2 m spacing (ERT1, ERT2, ERT3, ERT4) or 72 electrodes at 1 m spacing (ERT5, ERT6, ERT 7), and one small (SM) and one big (BM) passive 2D array consisting both of twelve seismic stations (equipped with three-components Lennartz-5s velocimeter) in a spiral-shape configuration.

The combination of the abovementioned investigations combined to provide the following preliminary geotechnical model (Figure 2b) for the liquefaction assessment at the Mirabello trial site:

- Topsoil "T" from 0 to 1 m bgl;
- Silty clay "SC" from 1 to 4 m bgl;
- Clayey silt with sand "CSS" from 4 to 6 m bgl;
- Silty sand and sandy silt (fluvial Apenninic coarse deposits) "SSA" from 6 to 8 m bgl;
- Silty sand (paleochannel of the Po River) "SSP" from 8 to 17 m bgl;
- Silty sand (Syn-Glacial braided Po River deposits) "SSSGP" from 17 to 20 m bgl.

Table 1 illustrates the geotechnical paramenters estimated for the model: corrected cone tip penetration resistance before (q_t) from CPTu test, horizontal stress index (K_D) from SDMT test, shear wave velocity (V_S) from SDMT and DH tests and fine content (FC) from sieve analyses.

Therefore, the preliminary CPT-based liquefaction analyses were integrated by additional analyses based on SDMT and DH data according to the "simplified procedure", assuming the same seismic input already used for CPTu liquefaction assessment. The liquefaction analyses based on the flat dilatometer test (DMT) were carried out using Monaco et al. [2005], Tsai et al. [2009] and Robertson [2012] formulations, while the analyses based on the shear wave velocity V_S were carried out according to the methods proposed by Andrus and Stokoe [2000] and Kayen et al. [2013]. The GWT was assumed equal to 4.2 m bgl. CPTu, DMT and V_S data found approximately the same potential liquefiable layers: the upper one, that is the main one, was detected between 6 and 8 m bgl corresponding to the fluvial Apenninic coarse-grained deposits (liquefaction safety factor $F_S \approx 0.6$-0.8), and the lower one, that is less liquefiable, between 8 and 13 m bgl into the upper paleochannel of the Po River ($F_S \approx 0.9$-1.2).

depth (m)	q_t (MPa)	K_D (-)	V_S (m/s)	FC (%)
0-1	0.5-1.5	20.0-45.0	85-105	-
1-4	0.8-1.8	4.5-17.5	135-160	100
4-6	0.3-1.1	3.0-4.0	140-170	70-80
6-8	0.8-2.0	1.5-3.0	155-170	25-75
8-17	6.0-11.5	3.0-6.0	170-215	20-35
17-20	13.0-18.0	3.5-6.0	200-225	-

Table 1: *Values of the corrected cone tip penetration resistance before (q_t), horizontal stress index (K_D), shear wave velocity (V_S) and fine content (FC) for the preliminary geotechnical model at Mirabello trial site.*

3.2. Blast test layout, site investigation and monitoring instrumentation

Based on the soil profile and liquefaction assessment, the blast layout was designed in February and March 2016.

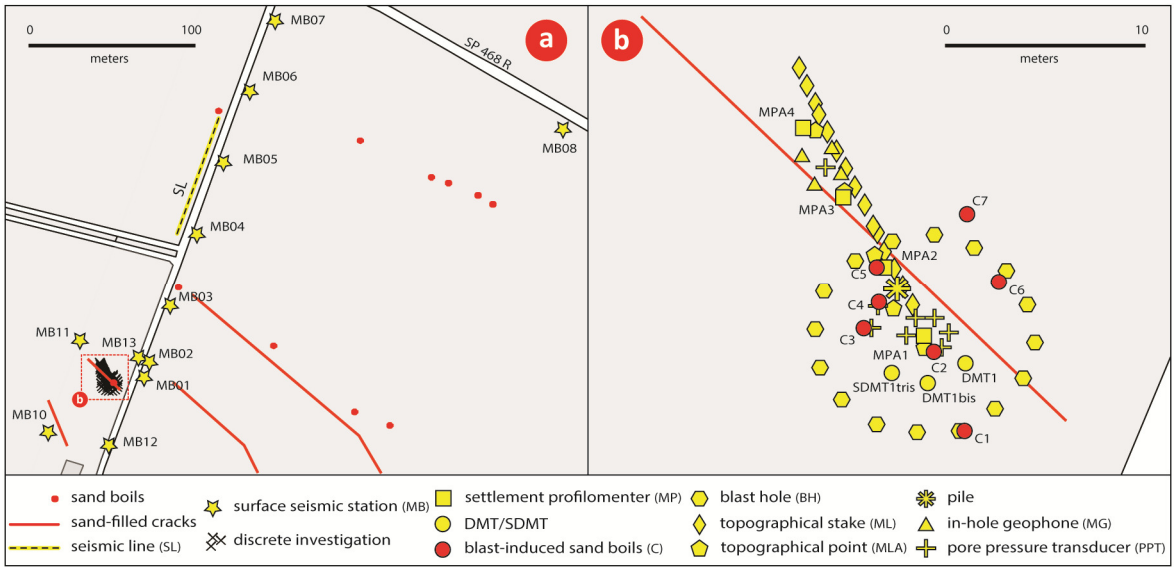

Figure 4. Map of blast investigations at the trial Mirabello blast test site.

Two sequences of blast charges were planned to detonate separately. For the first blast eight blast holes (BH) were equally distributed around a 5 m-radius circumference of a ring at 45°, and an offset of 22.5° for the second blast holes was adopted (Figure 4b). In each blast hole 1.875 kg and 2.5 kg charges were located in the potential liquefiable layers at 7.0 m bgl (fluvial Apenninic coarse deposits) and 11 m bgl (upper paleochannel of the Po River) depths respectively. This blasting plan provided an acceptable level of vibration for human perception and damage to building. The delay of detonations between each of the eight holes was fixed at 200 ms.

In order to evaluate ground behavior over the likely area of influence for the blasts, four additional companion soundings consisting of a 15 m-deep piezocone and a seismic dilatometer (CPTUA1-SDMTA1, CPTuA2-SDMTA2, CPTuA3-SDMTA3, CPTuA4-SDMTA4) were performed along the line of sand boils observed in the 2012 earthquake from the center of the blast ring to a 12 m radial distance (Figure 3b). Three supplementary boreholes (S2, S3, S4) and one piezometer (PZ1) were also planned in order to retrieve additional disturbed and undisturbed samples in the silty sands and sandy silt of the fluvial Apenninic coarse deposits and of the paleochannels of the Po Rivers, to carry out one extra 20 m-deep down-hole *Vs* test (DH2), and to monitor the ground water table (pink symbols in Figures 3a and 3b).

Four "Sondex" settlement profilometers (MPA1, MPA2, MPA3, MPA4) were located in correspondence with the four CPTu-SDMT pairs to monitor the vertical settlements as a function of depth soon after each blast sequence. The reference base was anchored at 18 m which corresponds with the most rigid and deepest silty sandy layer of the paleochannel of the Po River. Elevation measurements were also made with the level at five points (MLA, Figure 4b) within the blast zone to record the vertical

ground surface settlements over time after the blast. Moreover thirty-one stakes (ML, Figure 4b) were placed along a line out from the center of the blast zone to record the overall vertical settlements due to each blast using a survey level. These discrete point measurements were also coupled with detailed topographical surveys, by means of Terrestrial Laser Scanning (TLS), that allows an accurate and cost-effective representation of the topographical details of the observed surface, and Structure from Motion (SfM) aerial photogrammetry, that gives a highly automated registration of the images in the same reference frame by means of efficient feature-based or area-based matching techniques. The combinations of these topographical surveys provided very accurate and realistic 3D digital models of the investigated area (approximately a 20 m-diameter circle from the center of the blast zone), useful to monitor surface deformation via repeated surveys before and soon after each detonation.

The blast instrumentation layout also included a down-hole 3D (10 Hz) geophone array set up to record the blast signal. The array consisted of sensors (MG, Figure 4b) at each corner of a cube with side dimensions of about 1.5 m. The top four sensors were located near the top of the main liquefiable layer (6.3 m bgl) and the bottom four sensors near the bottom of the same layer (7.8 m bgl). The center of the array was settled 10 m from the center of the blast ring, estimating that at this distance the used geophones would not saturate during the detonations. Additionally thirteen surface seismic stations (MB, Figure 4a) equipped with a 24-bit digitizer (reftek) coupled to a velocimeter (Lennartz-5s) and an accelerometer (Episensor-1s), were placed between 20 m and 320 m from the blast center, to acquire the ground motion for each blast pulse. A linear array of 48 vertical (4.5 Hz) geophones at 1.5 m spacing (SL, Figure 4a) was also located on the surface about 150 m far from the blast center.

The installation of an instrumented micropile was additionally included in the blast test experiment (Figure 5) in order to improve the knowledge on the design of deep foundations in case of liquefaction.

Figure 5. Installation of the instrumented micropile.

The 250 mm diameter concrete test pile was reinforced with a 114 mm-diameter steel pipe with a 10 mm wall thickness internal reinforcement and was located 2.7 m from the center of the blast zone (Figure 4b). Based on CPTu2 data the micropile was designed to reach the upper paleochannel of the Po River at a depth of 17 m using overburden drilling. Strain gauges were installed at approximately 1.5 m depth intervals along the pile length to a depth of about 0.3 m above the bottom of the pile in order to measure the strain, and consequently calculate the load in the pile during the two blast sequences. In addition dynamic CASE load tests [Goble et al. 1967] were considered suitable to be performed on the pile to

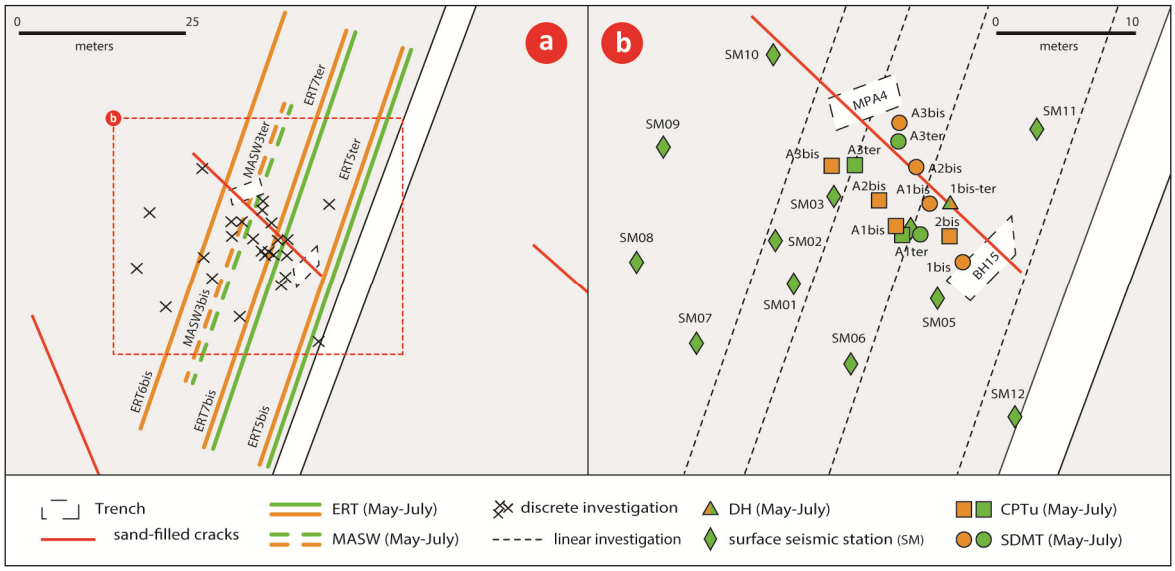

Figure 6. Map of post blast investigations at the trial Mirabello blast test site: orange color is related to the May site campaign, and green color indicates the July investigations.

evaluate the load-settlement curve and the distribution of shaft and base resistances of the pile before and after the detonations. CPTu2 data supported the evaluation of a 700 kg-weight falling through different distances (20 cm, 50 cm and 70 cm) to realize each CASE test.

Eight pore pressure transducers (PPT, Figure 4b) were located in the blast zone to monitor the generation and dissipation of excess pore pressure during the blasts. In particular, five piezometers were installed in the silty sandy layers that would be affected by the detonation at depths between 6 and 11 m bgl, typically about 1 m far from the center of the blast ring where the effect of the blast-induced pore pressure generation was expected to be maximum. Two additional PPTs were placed close to the pile to investigate the pore pressure behavior in the deepest silty sandy layers between 14 and 17 m bgl (bottom of the pile), and one supplementary PPT was located in the center of the 3D geophone array at roughly 7 m depth (average depth of the top and bottom sensors). Two flat dilatometer blades (DMT1 and DMT1bis) and a seismic dilatometer module (SDMT1tris) were placed at about a depth of about 7.2 m bgl (Figure 4b) to monitor the changes in horizontal stress and in shear wave velocity during and soon after the blast.

In April and May 2016 the supplementary boreholes, piezometer, CPTu, SDMT and DH tests were performed together with complementary compositional analyses in order to better characterize the blast zone before the detonations. In April 2016 the pile was constructed, while a month later the pre-blast CASE test was carried out. In May 2016 blast holes, profilometers, piezometers, DMT blades, SDMT module and in-hole geophones were also installed, while the explosive was charged the day of the blast tests, May 18, 2016. The equipment for both the discrete and areal topographical surveys

and the surface seismic stations were also placed the day of the blast tests. During and/or soon after each detonation each apparatus acquired data.

3.3. Post-blast site investigation

Two post blast site campaigns were planned at the end of May 2016 (orange lines and symbols in Figures 6a and 6b) and at the beginning of July 2016 (green lines and symbols in Figures 6a and 6b) in order to compare the variation with the time of the geotechnical and geophysical parameters before and after the blast experiment. In particular in May four 15-m deep seismic dilatometer tests (SDMTA1bis, SDMTA2bis, SDMTA3bis, SDMT1bis), four 15-m deep piezocone tests (CPTuA1bis, CPTuA2bis, CPTuA3bis, CPTu1bis), one 7 m-deep down-hole test (DH1bis), and one active and one passive seismic measurements (MASW3bis) and three geoelectrical surveys (ERT5bis, ERT6bis, ERT7bis) were executed using the same pre-blast configuration. Furthermore, in July a smaller site investigation was carried out with pairs of 15 m-deep SDMT-CPTu tests at A1ter and A3ter locations, a 7.5 m-deep DH test (DH1ter), and a geophysical surface surveys (MASW3ter, ERT5ter, ERT7ter, SMter passive 2D array). Two exploratory trenches (Figures 6a and 6b) were also excavated across the 2012 sand blows and almost orthogonal with respect to their mean strike, reaching a depth of about 2.0-2.5 m. The BH15 trench (8 m long) and the MPA4 trench (10 m long) were approximately 5 m and 12 m, respectively, from the blast center. These trenches were used to: a) identify possible deformational features (fractures and sand vents) related to the 2016 blast test (BH15 trench); b) characterize the fracture/conduit liquefaction features related to the 2012 earthquake (MPA4 trench); and c) identify and date possible paleoliquefaction events (historical and older, e.g 1570-74 Ferrara earthquakes) potentially recorded in the stratigraphic sequence exposed in both trench walls [De Martini et al. 2012]. In this respect sedimentological, petrographical and compositional analyses were also planned in order to improve the detail of the results in terms of identification and characterization of different stratigraphic units.

4. Preliminary results

4.1. Pre-blast results

The supplementary site investigation performed in April 2016 confirmed the preliminary geotechnical model obtained in January (Figure 2b). On average the topsoil "T" was confined between 0 and 1 m bgl, while the silty clay "SC" was encountered from 1 to 4 m bgl. The latter layer is highly plastic (plasticity index $PI \approx$ 31-58%), has a fine content $FC \approx 100$ % and contains a peaty layer (3.30-3.50 m bgl) that the radiocarbon datings (sample 330 Conventional age 1030±30 yr BP; sample 340 Conventional age 1080±30 yr BP, sample 330 2sigma calibrated age 900-1120 A.D.; sample 340 2sigma calibrated age 890-1020 A.D, calibration from Reimer et al. [2013]).attributed to 890-1120 AD [Servizio Geologico Sismico e dei Suoli, Regione Emilia-Romagna 2016]. The clayey silt with sand "CSS" was plastic ($PI \approx$ 23-27 %), had a high $FC \approx$ 70-80 %, and was approximately confined between 4 and 6 m bgl. The fluvial Apenninic deposits "SSA" were composed of silty sand and sandy silt with low plasticity ($PI \approx$ 5-9 %) and $FC \approx$ 25-75 %, and were roughly detected from 6 to 8 m bgl. Finally two different paleochannels of

the Po River, both composed of non-plastic silty sand, were found: the upper one "SSP" from 8 to 17 m bgl (*FC* ≈ 20-35 %), and the lower one "SSSGP" from 17 to 20 m bgl. ERT profiles also confirmed this geotechnical model, as shown in Table 2. Besides the relatively higher values of electrical resistivity ρ in the surficial dry crust "T", the fine-grained deposits (i.e. "SC" and "CSS") provide low resistivities (ρ ≈ 6-14 Ohm·m). The lower values can be related to the presence of the ground water table located, at the time of ERT execution (February 2016), at GWT ≈ 4.2 m bgl. In contrast the coarse sediments (i.e. "SSA", "SSP" and "SSSGP") detect higher resistivities (ρ ≈ 10-33 Ohm·m), with the ρ value increasing approximately as the fine content decreases.

z (m)	ρ_{pre} (Ohm·m)	$\rho_{post\ May}$ (Ohm·m)	$\rho_{post\ July}$ (Ohm·m)
0-1	30-40	11-15	10-14
1-4	10-14	6-10*	6-10
4-6	6-10	6-10*	6-10
6-8	10-20	5-15*	8-18
8-15	22-33	10-20*	15-25

*Lost of lateral continuity

Table 2: *Average values of the electrical resistivity before (ρ_{pre}) and after (May: $\rho_{post\ May}$; July: $\rho_{post\ July}$) the blast test.*

The following tables summarize the average pre-blast geotechnical and geophysical parameters obtained for the various soil layers, in terms of corrected cone tip resistance q_t (Table 3) from CPTu tests, horizontal stress index K_D (Table 4) and constrained modulus *M* (Table 5) from SDMT tests, and shear wave velocity V_S (Table 6) from DH, MASW and SDMT.

depth (m)	$q_{t\ pre}$ (MPa)	$q_{t\ post\ May}$ (MPa)	$q_{t\ post\ July}$ (MPa)
0-1	0.5-1.5	-	0.4-0.8
1-4	0.8-1.8	0.7-1.6	0.7-1.6
4-6	0.6-1.1	0.4-0.9	0.6-1.0
6-8	0.6-2.5	0.5-2.0	0.8-2.1
8-17	6.0-11.5	4.5-11.0	5.5-11.0
17-20	13.0-18.0	-	-

Table 3: *Average values of the corrected cone tip penetration resistance before ($q_{t\ pre}$) and after (May: $q_{t\ post\ May}$; July: $q_{t\ post\ July}$) the blast test.*

depth (m)	$K_{D\ pre}$ (-)	$K_{D\ post\ May}$ (-)	$K_{D\ post\ July}$ (-)
0-1	15.0-50.0	10.0-40.0	15.0-45.0
1-4	4.5-17.5	3.5-12.0	4.5-13.0
4-6	2.0-4.5	1.5-3.0	2.5-4.5
6-8	1.5-3.5	1.0-2.5	1.5-3.0
8-17	2.5-6.5	1.5-5.0	2.0-6.0
17-20	3.5-5.0	-	-

Table 4: *Average values of the horizontal stress index before ($K_{D\ pre}$) and after (May: $K_{D\ post\ May}$; July: $K_{D\ post\ July}$) the blast test.*

The high variation of V_S values within each layer can be attributed to the use of both invasive and non-invasive techniques. For example, the MASW tests can includes some uncertainties in the non-univoque process of the inversion step from the dispersion curve to the V_S profile and have to be related to a

wider investigation volumes than in-hole tests, such as DH or SDMT [Garofalo et al. 2016] therefore higher variability is expected.

depth (m)	M_{pre} (-)	$M_{post\ May}$ (-)	$M_{post\ July}$ (-)
0-1	10.0-30.0	6.0-20.0	10.0-22.0
1-4	15.0-40.0	12.0-30.0	13.0-30.0
4-6	3.0-8.0	2.0-8.0	2.5-8.0
6-8	2.0-20.0	2.0-15.0	3.0-20.0
8-17	25.0-85.0	20.0-60.0	25.0-60.0
17-20	55.0-90.0	-	-

Table 5: *Average values of the constrained modulus (M_{pre}) and after (May: $M_{post\ May}$; July: $M_{post\ July}$) the blast test.*

depth (m)	$V_{S\ pre}$ (m/s)	$V_{S\ post\ May}$ (m/s)	$V_{S\ post\ July}$ (m/s)
0-1	75-115	70-90	65-95
1-4	120-180	85-125	100-130
4-6	120-170	100-140	110-150
6-8	140-170	115-160	130-180
8-17	160-260	140-240	155-260
17-20	200-260	220 - 270	235 - 275

Table 6: *Average values of the shear wave velocity before ($V_{S\ pre}$) and after (May: $V_{S\ post\ May}$; July: $V_{S\ post\ July}$) the blast test.*

Moreover, the variability of the topsoil and "SC" layer parameters is also due to seasonal variations in water content along with fluctuation of the GWT. During the 2015-2016 dry season (from summer time up to February 2016), the presence of a shallow desiccation crust (GWT ≈ 4.2 m) was observed that changed its mechanical properties when rainfall increased (from April 2016 GWT measured by PZ1 ≈ 3.2 m).

According to the preliminary liquefaction potential assessment the low values of resistance (q_t ≈ 0.6-2.5 MPa, K_D ≈ 1.5-3.5) and stiffness (M ≈ 2.0-20.0 MPa, V_S ≈ 140-170 m/s) in the silty sand and sandy silt "SSA" confirmed the high liquefaction susceptibility of the fluvial Apenninic coarse deposits. After the upper paleochannel of the Po River "SSP" is encountered, the liquefaction confirmed of the silty sands starts to decrease until the highest values of the liquefaction safety factor (F_S > 1.2) are encountered in the Syn-Glacial braided Po River deposits "SSSGP" (q_t ≈ 13.0-18.0 MPa, K_D ≈ 3.5-5.0, M ≈ 55.0-90.0 MPa, V_S ≈ 200-260 m/s).

Whereas the MASW linear arrays derive a dispersion curve in the high-frequency range (from 8 to 25 Hz with apparent phase velocity spanning from 150 to 85 m/s), the passive 2D arrays are able to investigate the dispersion properties in a lower range of frequencies (1.2-5 Hz and 4-15 Hz for the big and small 2D array, respectively). The combined dispersion curves based on array analysis, together with the ground motion recorded by the accelerometers during the blast shots, will be presented in a next specific paper. Further, the microtremor data recorded by the seismic stations within the 2D arrays were also used to compute the H/V noise spectral ratios [Nakamura 1989, Milana et al. 2014]. The H/V ratios detect two low amplification frequency peaks likely related to the deepest layers not investigated by the other geotechnical and geophysical tests: the first one at about 0.7 Hz may refer to the impedance contrast (≈ 80-100 m bgl) between the Bazzano Subsynthem (AES6)

and the undifferentiated portion of the Upper Emiliano-Romagnolo (AESi), while the second spectral H/V peak at about < 0.3 Hz may correspond to the impedance contrast (≈ 800 m bgl) between the Marine Quaternary (QM) and the Middle-Upper Pliocene (P2). A third dubitative peak is also present at 0.17 Hz near to the eigenfrequency of the velocimeter (0.2 Hz) and could be related to a deeper contact between Pliocene–Quaternary deposits and Miocene marls [Mascandola et al. 2016]. Further details on the abovementioned stratigraphical units can be found in Minarelli et al. [2016].

Compositional analyses of sands in the pre-blast conditions were performed on the 0.125–0.250 mm fraction, according to the Gazzi–Dickinson method, in order to reduce the effect of grain size over composition [Lugli et al. 2007, Weltje 2002]. The examined sands are characterized by well-defined fields and show a clear trend from lithoarenitic to quartz-feldspar-rich compositions, similar to that evidenced by Fontana et al. [2015]. In detail:

- sands from "CSS" deposits represent a very subordinate fraction. They are the most lithoarenitic, with shales as the dominant lithic type. Quartz plus feldspars range from 52.9 % to 58.0 % of the whole sandy fraction. Siliciclatic fine-grained lithics (shale, siltstones, low-grade metamorphites) vary from 19.0 % to 24.0 % and carbonate lithics (sparitic and micritic limestones, calcite spars) range from 13.8 % to 14.4 %. Micas, glauconitic grains, heavy minerals and Fe-oxides are subordinate components;
- sands from "SSA" show a composition similar to the "CSS" level, but slightly enriched in quartz and feldspars (up to 63.0 %) and impoverished in siliciclastic lithic fragments (13.7-19.4%);
- sands from "SSP" clearly differ in composition and show a higher quartz-feldspar content. In detail this layer has quartz and feldspars from 69.7 % to 74.7 %, siliciclastic fine-grained lithics from 8.3 % to 11.6 % and carbonate lithics from 9.9 % to 14.1 %;
- compositional field of deepest sands "SSSGP" overlap the one of "SSP" sands, but with higher amounts of quartz (single crystal) and lower of shales.

The shifting composition at 8 m depth is interpreted as the transition from Apenninic to Alpine provenance of the deeper Po river sands.

Finally, a pre-blast dynamic CASE load test on the test micropile was performed on May 2016. The results are illustrated in terms of axial resistence and load-settlement curves due to the uncertanties and the factors that may affect the end bearing capacity interpreted from the CASE test and the CAPWAP (CAse Pile Wave Analysis Program) results. Before the blast the CASE test yielded a shaft resistance of 630 kN, developed from the uppermost part of the subsoil to around 11 m bgl where the values strongly decreased. In terms of load-settlement curve the CASE test had a very stiff response that however was not possible to reproduce using the site characterization. This may be in part due to the fact that the CASE test was not calibrated based on a static load test and also the fact that the pile was probably able to manifest a stiffer response than predicted.

4.2. Blast results

On the 18th May 2016 the two sequences of blast charges were detonated separately. The

first one followed the planned configuration, while for the second one the charges in each hole were reduced to 2.5 kg and located at approximately 6 m bgl. Nevertheless, the generation and the dissipation of the excess pore water pressure (i.e. pressure in excess of static water pressure) were similar in both the blast events, as measured by PPTs. With each charge detonation a transient pulse was produced which led to a progressive increase in the pore pressure ratio R_u (ratio between the excess pore pressure and the initial vertical effective stress) until complete (or almost complete) liquefaction was achieved with R_u values of about 0.8-1.0 between 6 and 10 m bgl. For the first blast, as confirmed also by DMT data, approximately after 15 minutes R_u returned below 0.1, whereas this occurred in about 10 minutes for the second detonation.

Liquefaction was also proved by the presence of seven sand boils (Figure 7) around the test area (C1 to C7, Figure 4b), that were sampled for granulometric and compositional analyses. Preliminary laboratory information detected that the blast-induced level belongs to the fluvial Apenninic coarse deposits.

Figure 7. Blast-induced sand boils after the first detonation.

The in-hole 3D geophone array, the surface array of 48 vertical geophones and the thirteen velocimeters saturated during both the blast sequences, while all the accelerometers properly acquired the data for each pulse. For the first detonation the Mirabello surface vibration data show horizontal and vertical peak ground accelerations (*PGA*) of about 0.60 g and 1.70 g, respectively, at 20 m from the center of the blast zone. Due to the smaller charges, the second blast recorded lower PGA values that are approximately equal to 0.36 g and 0.55 g for horizontal and vertical components, respectively, at 20 m from the center of the blast zone. In both cases the blast-induced ground motion attenuated rapidly with distance, and the vertical component reached values smaller than 0.15 g (first blast) and 0.05 g (second blast) about 100 m distance.

Velocity time histories were also determined for each component by integrating the acceleration time histories. The *PPV* parameter provides an exponentially decreasing trend, consistent with other field tests [Kato et al. 2015]. *PPV* shows similar values for the first and second shots of the blast experiment. Indeed for both shots the seismic station situated at 20 m from the center of the blast zone shows a *PPV* of approximately 0.09 and 0.02 m/s (for horizontal and vertical component, respectively). *PPV* values decrease at 100 m far at 0.015 (vertical component) and 0.007 m/s (horizontal component).

Despite the rectangular form and the small size of the nearly flat area of Mirabello trial site, TLS and SfM analyses aimed to obtain soil deformation via multi-temporal models and model comparison were not simple. Strong limitations were indeed imposed due to the presence of several participants and instruments in the blast area occluding

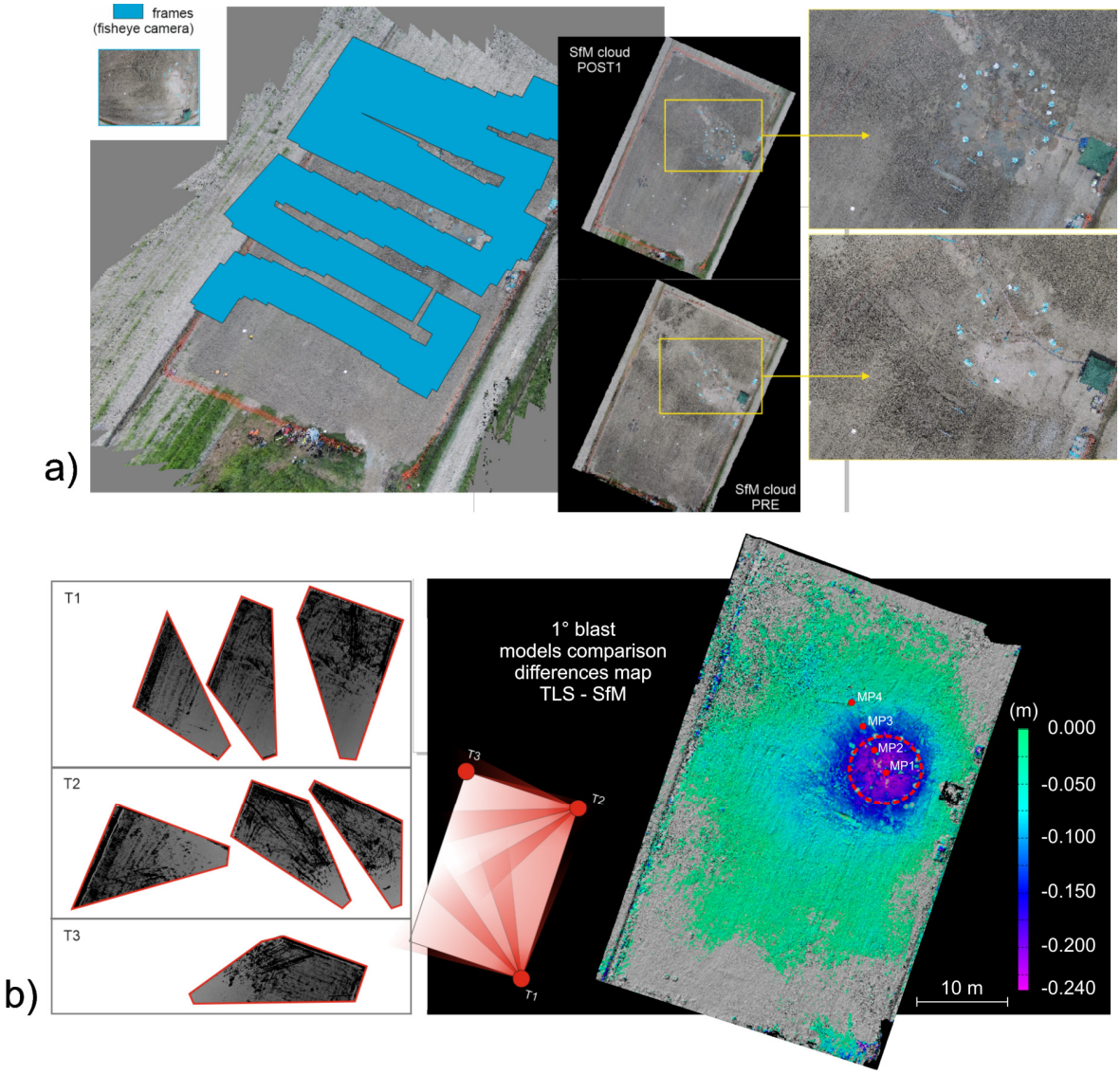

Figure 8. TLS and SfM methodologies to observe and measure surface displacements. (a) The images were acquired using flying drone, frames and camera position in the space; the point clouds were obtained from data analysis using Phostoscan software. (b) The TLS point clouds were acquired scanning from three station points (Ti) and model reconstruction, while map of differences was obtained by comparing multitemporal models before and after the first blast.

targets. Therefore, the reconstruction of a detailed final model was incomplete over the area. Nevertheless, results of the analyses clearly describe a 10 m-diameter circular deformed area settling toward the center (Figure 8). Polyorks (Innovmetrics) and Photoscan software (AgiSoft) where used for data processing. In Figure 8 values refer to vertical displacements, and the contouring map clearly describes a pattern where the

mainly differences are contained into a circular area (red dashed line). After the first blast the ground surface subsided about 15-20 cm (and more) providing a pattern clearly visible and centered in the zone where detonation occurred. Soil settlements decrease with the distance reaching negligible values at 10 m from the center of the blast zone. The test pile settled about 1.5-2.0 cm. After the second blast a pattern similar to the one observed in Figure 8 was observed: a circular 20 m diameter zone was involved showing maximum vertical displacements of about 10-12 cm. Additional models are ongoing and will be provided in next works after repeatability tests in order to overcome possibly systematic errors. The test pile showed no movement at all.

Finally the high details of models from remote sensing allowed to extract punctual data in correspondence of the profilometers: after the first blast relevant surface settlements of about 20-22 cm, 18-20 cm, 12-14 cm and 4-6 cm were estimated in correspondence of MPA1, MPA2, MPA3 and MPA4, respectively (see Figure 8).

The general findings of the discrete ground surface soil settlement measurements met expectations with the maximum amount of subsidence of 34 cm occurring in the center of the blast zone (first blast: 19 cm; second blast: 15 cm). As the distance from the center of the blast zone increased, the settlement amounts recorded decreased, and the highest settlements were recorded within the blast circle. Due to preconsolidation, the settlement after the second blast was less even though the recording interval was longer (roughly 13 hours compared to 5 hours). Both detonations display similar settlement curves. These curves represent the dissipation of the excess pore pressure that developed during the liquefaction phase. As the pore pressures decreased, the settlement increased. In additions, some creep settlement may occur after pore pressures are dissipated as the sand moves into the denser arrangement.

Similar to the discrete ground surface settlement data, the discrete settlement data with respect to depth decreased as the distance from the center of the blast zone increased, and the highest settlements were recorded within the blast circle. Figure 9 illustrated the profilometer test results after the first blast: vertical ground displacements were measured equal to 19 cm at MPA1, 16.5 cm at MPA2, 6.7 cm at MPA3 and 2.2 cm at MPA4, and they provided a reasonable agreement when compared also with the areal topographical surveys.

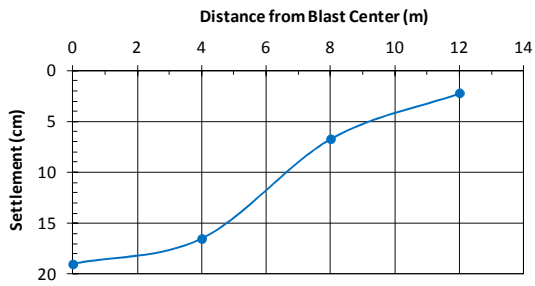

Figure 9. Profilometer test results after the first blast.

Moreover the profilometer at the center of the blast zone (MPA1) recorded a combined settlement of about 36 cm after the detonations, and 38 cm one week after the blasts. Most of the consolidation with respect to depth occurred in the liquefied layers and layers with elevated pore pressures between 6 and 12 m bgl.

Pile data interpretation is still ongoing, however, some preliminary observations are possible. Blast-induced liquefaction led to negative skin friction and pile settlement.

Negative friction in the cohesive soil layers above 6 m was similar to the positive friction based on the undrained shear strength and that from the CASE test. As the liquefied layer settled owing to dissipation of excess pore pressures, the increased effective stress allowed negative skin friction to progressively increase at the silty sand and sandy silt-pile interface. Similar to previous full-scale blast liquefaction tests [Rollins and Hollenbaugh 2015, Rollins and Strand 2006] the Mirabello results suggests that after consolidation, the average skin friction in liquefied layer was 30 to 50 % of the pre-liquefaction skin friction.

4.3. Post-blast results

The representative values of the post-blast geotechnical and geophysical parameters measured in the two site campaigns (May 2016 and July 2016) are reported in Tables 2, 3, 4, 5, 6. The corrected cone resistance q_t (Table 3), the horizontal stress index K_D (Table 4), the constrained modulus M (Table 5), and shear wave velocity V_S (Table 6) evidenced a reduction in soil resistance and stiffness within the liquefied layer of the fluvial Apenninic coarse silty sands and sandy silt after the execution of blast tests, that was partially recovered with time. A certain decrease is also detectable in the silty sand layer of the upper paleochannel of the Po River. In addition ERT surveys (Table 2) observed a reduction in electrical resistivity in the same liquefied layer after blast tests and a similar partial recover with time. A similar resistivity variation was observed also within the lower silty sandy layer. Imaged resistivity differences from one of the ERT surveys, within the interested layers in the blast zone are reported in Figure 10. The observed variations can be related to changes in the compaction of the interested layers. In both the layers also a variation in the lateral continuity of the layers can be observed in the tomograms after blast tests. However all the tests also indicate a reduction in the values of resistence and stiffness parameters (ρ, q_t, K_D, M, V_S) in the upper 6 m bgl, probably due to the tendency to rise of the liquefied silty sand and sandy silt through the surface.

The July post-blast CASE test on the pile provided very similar results when compared to the pre-blast CASE test in terms of axial resistance (630 kN). Nevertheless, after the detonations the first 7 m of pile became practically ineffective in developing lateral resistance that was instead transferred entirely to the deeper section of the pile (the last 10 m). A similar trend was visible from the May post-blast CASE test that yielded a much lower shaft resistance (491 kN). Moreover the post-blast CASE tests showed how the pile-soil interaction is decidedly less rigid due to induced liquefaction. These results can be explained by the blast-induced liquefaction that initially decreased soil resistance and stiffness, but these properties partially recovered with time as confirmed by the post-blast site campaigns.

At the end of July 2016 exploratory trenches, 2.0-2.5 deep, were also dug (see Figure 6 for their location). The trench walls were first cleaned, then a regular grid was applied and a set of detailed pictures was taken to better record the nature of the deposits and the sedimentary/deformation-structures that were exposed. This data set was then used to derive high resolution trench photomosaics from SfM image-based modeling. A stratigraphic log (Figure 11) was drawn at 1:20 scale evidencing: a) a reworked layer at the surface related to post-2012 plowing and to set up activities for the blast test (unit A:

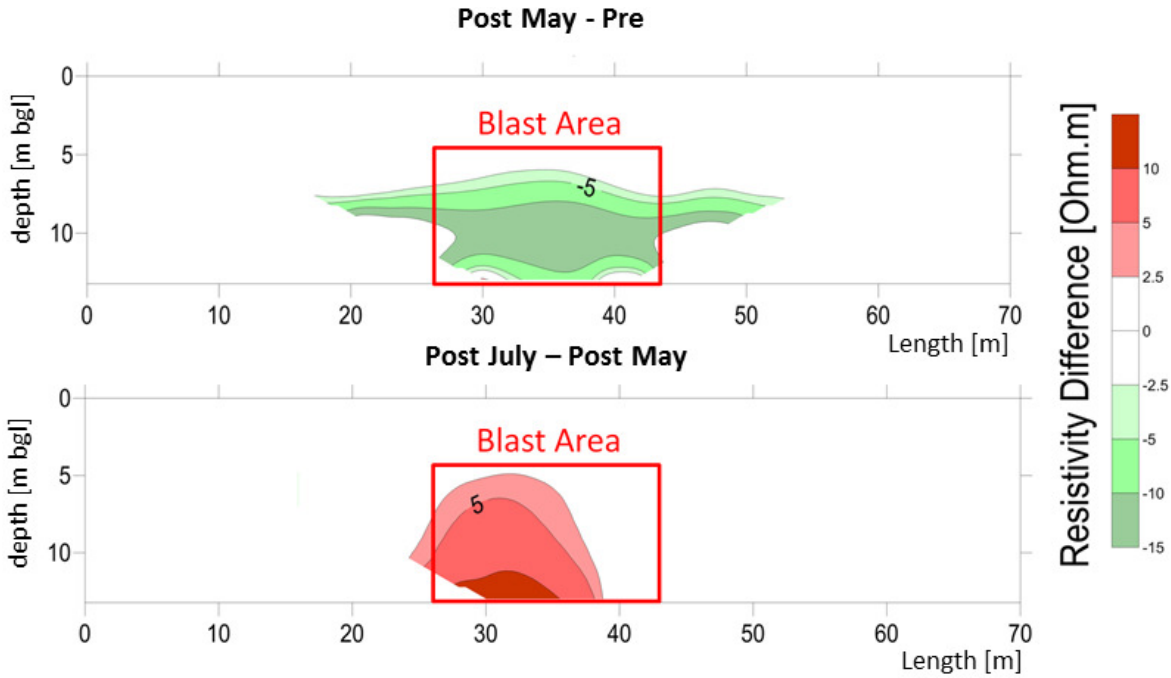

Figure 10. Imaged resistivity differences (from top to bottom Post-May minus Pre-February and Post-July minus Post May) from one of theERT surveys, within the fluvial Apennines coarse deposits and the upper paleochannel of the Po River in the blast zone.

plowed horizon and 2012 sands mixed up); b) a sedimentary sequence dominated by hazel to brown silt to clay deposits of fluvial origin (mainly overbank sediments, see Figure 11), usually massive with only one laminated clayey layer (unit D); and c) several fractures, up to a few cm wide and almost vertical, that were filled by medium to fine grey sand, reaching the 2012 sand blow layer, up to 25 cm thick (unit S in Figure 11). Several sediment samples were collected from the trench walls (Figure 11).

Sedimentological, compositional and petrographical analyses are in progress, with particular attention to the sands collected from different fractures and from the 2012 sand blow on the trench walls. However, some preliminary observations can be provided. The trench walls show the presence of several fractures used by the liquefied sands in 2012 to reach the surface. These fractures are responsible for producing the multiple aligned sand volcanos investigated. The ongoing analyses will help in identifying and discriminating between the 2012 event sand and those of different origin possibly related to the blast test or to older liquefaction phenomena.

5. Conclusions

A full-scale blast-induced liquefaction test was carried out for the first time in Italy following the 2012 Emilia earthquake. The controlled blasting experiment was successful in inducing liquefaction in a well-defined volume of soil in the trial field site of the Mirabello village.

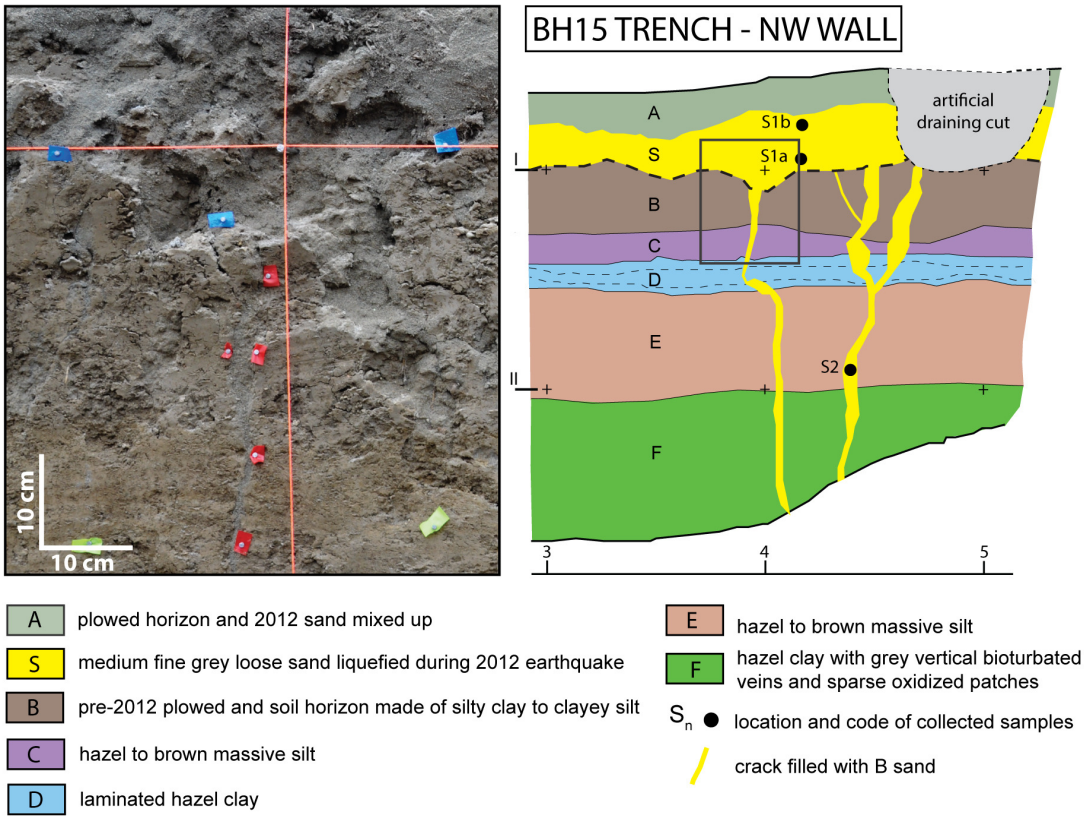

Figure 11. Detail of the NW wall of the BH15 trench (see Figures 2e and 2f for location): Detail of the 2012 sand conduit (left; see black frame on the log) and interpreted log (right) of the 3-5 meter section.

Pre- and post-blast in-depth site investigation allowed to thoroughly characterize the site and to observe the effects produced by the blast induced liquefaction.

The measurements of excess pore pressures and soil deformations were used to locate the liquefied layers, that correspond to the fluvial Apenninesic coarse deposits (6-8 m bgl) and to the upper part of a paleochannel of the Po River (8-12 m bgl).

Peak ground motion parameters (*PPV* and *PGA* values) attenuated rapidly from the center of the blast zone, and their trends are generally in agreement with the previous case studies.

Blast-induced liquefaction and resulting soil settlement produced negative skin friction on test pile that led to pile settlement. Negative friction was similar to the pre-blast friction in the cohesive surface layers but was reduced to 30 to 50% of the pre-blast value in the liquefied sand layers.

The comparison between the pre-blast and post-blast soil parameters highlighted a reduction in soil resistance and stiffness

within the liquefied layers after the blast. Such reduction was partially recovered with time (two months later). Invasive and non-invasive tests also showed a reduction in some test and soil parameters (tip cone resistance q_t from CPTu tests; horizontal stress index K_D and constrained modulus M from SDMT; shear wave velocity V_S from SDMT, MASW and DH test) in the upper 6 m bgl probably due to the tendency for the stiff clay to crack and allow the liquefied silty sand and sandy silt to rise to the surface.

The partial loss and recovery of mechanical soil properties is supported also by the CASE test results, that after the detonations showed an ineffectiveness of the pile to develop shaft resistance in the upper 7 m, and a softer pile load-deflection curve due to the blast-induced liquefaction.

6. Acknowledgements

The study was mainly funded by FIRB-Abruzzo project ("Indagini ad alta risoluzione per la stima della pericolosità e del rischio sismico nelle aree colpite dal terremoto del 6 aprile 2009", http://progettoabruzzo.rm.ingv.it/it).

Special thanks to Brigham Young University for contributing to the realization of the blast test experiment in terms of personnel and technical equipment; to Geoconsult srl (Giuseppe Miceli) that partially financed the CASE tests; to the technicians from differents Universities and Companies (Dave Anderson, Andrew Sparks, Roberto Bardotti, Giovanni Bianchi, Diego Franco, Constantin Diaconu) that helped in the execution and elaboration of the geotechnical and geophysical tests.

A special thank also to the Mirabello Municipality (in particular the mayor Angela Poltronieri) that made this experiment possible in collaboration with the other local authorities (Ferrara Prefecture, Emilia-Romagna Region, Ferrara Province, Local Civil Protection, Police, Fire Brigade).

References

Amorosi, A., Bruno, L., Cleveland, D.M., Morelli, A. and Hog W. (2016). Paleosols and associated channel-belt sand bodies from a continuously subsiding late Quaternary system (Po Basin, Italy): New insights into continental sequence stratigraphy, Geological Society of America Bulettin, doi: 10.1130/B31575.1

Andrus, R.D. and Stokoe, K.H. (2000). Liquefaction resistance of soils from shear-wave velocity, J. Geotech. Geoenviron. Eng, ASCE 126 (11): 1015-1025.

Ashford, S., Rollins, K. and Lane, J. (2004). Blast-induced liquefaction for full-scale foundation testing. Journal of Geotechnical and Geoenvironmental Engineering, 130(8), 798–806.

Bruno, L., Amorosi, A., Severi, P. and Costagli, B. (2016). Late Quaternary aggradation rates and stratigraphic architecture of the southern Po Plain, Italy, Basin Research, doi:10.1111/bre.12174

Caputo, R. and Papathanasiou, G. (2012). Ground failure and liquefaction phenomena triggered by the 20 May,

2012 Emilia-Romagna (Northern Italy) earthquake: case study of Sant'Agostino - San Carlo - Mirabello zone, Natural Hazards and Earth System Sciences, vol. 12, no. 11, pp. 3177-3180, doi: 10.5194/nhess-12-3177-2012.

De Martini, P. M., Cinti, F.R., Cucci, L., Smedile, A., Pinzi, S., Brunori, C.A. and Molisso, F. (2012). Sand volcanoes induced by the April 6th 2009 Mw 6.3 L'Aquila earthquake: a case study from the Fossa area, Italian, J. Geosci., 131, 410–422.

Emergeo Working Group (2013). Liquefaction phenomena associated with the Emilia earthquake sequence of May-June 2012 (Northern Italy), Natural Hazards and Earth System Sciences, 13 (4), 935-947; doi: 10.5194/nhess-13-935-2013.

EN 1998-5 (2004). Eurocode 8: Design of structures for earthquake resistance - Part 5: Foundations, retaining structures and geotechnical aspects, CEN European Committee for Standardization, Bruxelles, Belgium.

Facciorusso, J., Madiai, C. and Vannucchi, G. (2016). The 2012 Emilia earthquake (Italy): geotechnical characterization and ground response analyses of the paleo-Reno river levees. Soil Dynamics and Earthquake Engineering, Vol. 865, 71-88, doi:10.1016/j.soildyn.2016.04.017

Finno, R.J, Gallant, A.P. and Sabatini, P.J., (2016). Evaluating Ground Improvement after Blast Densification at the Oakridge Landfill, Journal of Geotechnical and Geoenvironmental Engineering, ASCE, Vol. 142, No. 1, 2016, 04015054, 1-13.

Fioravante, V., Giretti, D., Abate, G., Aversa, S., Boldini, D., Capilleri, P., Cavallaro, A., Chamlagain, D., Crespellani, T., Dezi, F., Facciorusso, J., Ghinelli, A., Grasso, S., Lanzo, G., Madiai, C., Massimino, M. R., Maugeri, M., Pagliaroli, A., Ranieri, C., Tropeano, G., Santucci De Magistris, F., Sica, S., Silvestri, F. and Vannucchi, G. (2013). Earthquake geotechnical engineering aspects: the 2012 Emilia-Romagna earthquake (Italy), Seventh International Conference on Case Histories in Geotechnical Engineering, Chicago, 1-34.

Fontana, D., Lugli, S., Marchetti Dori, S, Caputo, R. and Stefani M. (2015). Sedimentology and composition of sands injected during the seismic crisis of May 2012 (Emilia, Italy): clues for source layer identification and liquefaction regime, Sedimentary Geol, 325, 158-167.

Garofalo, F., Foti, S., Hollender, F., Bard, P.Y., Cornou, C., Cox, B.R., Dechamp, A., Ohrnberger, M., Perron, V., Sicilia, D., Teague, D. and Vergniault, C. (2016). InterPACIFIC project: Comparison of invasive and non-invasive methods for seismic site characterization. Part II: Inter-comparison between surface wave and borehole methods, Soil Dynamics and

Earthquake Engineering, 82, 241-254, doi:10.1016/j.soildyn.2015.12.009.

Geotema (2014). Microzonazione sismica Livello 2 con locali approfondimenti di Livello 3, Regione Emilia-Romagna. Comune di Mirabello (FE), Relazione illustrativa e 7 tavv. (in Italian). http://www.comune.mirabello.fe.it/files/00036/relazione_ms_mirabello.pdf

Goble, G.G., Scanlan, R.H. and Tomko, J.J. (1967). Dynamic studies on the bearing capacity of piles, Final project Report, Division of Solid Mechanics Structures and Mechanical Design School of Engineering Case Western Reserve University, Cleveland, OH.

Gohl, W.B., Howle, J.A. and Rea, C.E. (2001). Use of controlled detonation of explosives for liquefaction testing, Fourth International Conference on Recent advances in Geotechnical Earthquake Engineering and Soil Dynamics and Symposium in Honor of Professor W.D. Liam Finn, San Diego, California, March 26-31, 2001.

Győri, E., Tóth, L., Gráczer, Z. and Katona, T. (2011). Liquefaction and post-liquefaction settlement assessment - A approach. Acta Geodaetica et Geophysica Hungarica 46(3): 347–369, doi:10.1556/AGeod.46.2011.3.6

Idriss, I.M. and Boulanger, R.W. (2008). Soil liquefaction during earthquakes. EERI Report, Publ. No. MNO-12, Earthquake Engineering Research Institute.

Ishihara, K. and Yoshimine, Y. (1992). Evaluation of settlements in sand deposits following liquefaction during earthquakes, Soils and Foundations, 32(1): 173-188.

Iwasaki, T., Tokida, K., Tatsuoka, F., Watanabe, S., Yasuda, S. and Sato, H. (1982). Microzonation for soil liquefaction potential using simplified methods. Proc. of 3rd Int. Conf. on Microzonation, Seattle, 3, 1319–1330.

Kato, K., Mason, H.B. and Ashford, S.A. (2015). Ground vibration fromblast-induced liquefaction testing from Christchurch, New Zealand, 6ICEGE – 6th International Conference on Earthquake Geotechnical Engineering, 1-4 November 2015, Christchurch, New Zealand.

Kayen, R., Moss, R., Thompson E., Seed, R., Cetin, K., Kiureghian, A., Tanaka, Y. and Tokimatsu, K. (2013). Shear-wave velocity-based and deterministic assessment of seismic soil liquefaction potential, J. Geotech. Geoenviron. Eng., ASCE 2013, 139(3): 407-419.

Kramer, S.L. (1996). Geotechnical Earthquake Engineering. Prentice Hall.

Lugli, S., Marchetti Dori, S. and Fontana, D., (2007). Alluvial sand composition as a tool to unravel the Late Quaternary sedimentation of theModena Plain, northern Italy. In: Arribas J., Critelli, S., Johnsson, M.J. (Eds.), Sedimentary Provenance and Petrogenesis: Perspectives from Petrography and

Geochemistry. Geological Society of America Special Paper, 420, 57–72.

Mascandola, C., Massa, M., Barani, S., Lovati S., and Santulin, M. (2017). Long-Period Amplification in Deep Alluvial Basins and Consequences for Site-Specific Seismic-Hazard Analysis: An Example from the Po Plain (Northern Italy), Bulletin of Seismological Society of America, doi: 10.1785/0120160166.

Milana, G., Bordoni, P., Cara, F., Di Giulio, G., Hailemikael, S., and Rovelli, A. (2014). 1D velocity structure of the Po River plain (Northern Italy) assessed by combining strong motion and ambient noise data, Bulletin of Earthquake Engineering, 12(5), 2195-2209.

Minarelli, L., Amoroso, S., Tarabusi, G., Stefani, M. and Pulelli, G. (2016). Down-hole geophysical characterization of middle-upper Quaternary sequences in the Apennine Foredeep, Mirabello, Italy, Annals of Geophysics, ISSN: 2037-416X, 59(5), S0543, doi:10.4401/ag-7114

Monaco, P., Marchetti, S., Totani, G. and Calabrese, M. (2005) Sand liquefiability assessment by Flat Dilatometer Test (DMT), Proc. XVI ICSMGE, Osaka, 4: 2693-2697.

Nakamura, Y. (1989). A method for dynamic characteristics estimation of subsurface using microtremors and the ground surface, Q. Rept. RTRI Japan, 30, 25-33.

Optech (2015). ILRIS 3D laser scanner description, http://www.optech.com/index.php/product/optech-ilrisi (Oct. 16, 2015).

Pyke, R., Seed, H.B. and Chan, C.K. (1975). Settlement of sands under multidirectional shaking, Journal of the Geotechnical Engineering Division 101(4):379-398.

Regione Emilia-Romagna (2012). Carta degli effetti di liquefazione osservati dopo i terremoti del 20 e 29 Maggio 2012, http://geo.regione.emilia-romagna.it/gstatico/documenti/liq2012/MAPPA_LIQUEFAZIONI_01.pdf

Regione Emilia-Romagna (2013). Sisma 2012 - Studi sismici, Ordinanza n. 70 del 13/11/2012 e cartografia di riferimento (in Italian), http://ambiente.regione.emilia-romagna.it/geologia/temi/sismica/speciale-terremoto/sisma-2012-ordinanza-70-13-11-2012-cartografia

Reimer, P.J., Bard, E., Bayliss, A., Beck, J.W., Blackwell, P.G., Bronk Ramsey, C., Buck, C.E., Cheng, H., Edwards, R.L., Friedrich, M., Grootes, P.M., Guilderson, T.P., Haflidason, H., Hajdas, I., Hatté, C., Heaton, T.J., Hogg, A.G., Hughen, K.A., Kaiser, K.F., Kromer, B., Manning, S.W., Niu, M., Reimer, R.W., Richards, D.A., Scott, E.M., Southon, J.R., Turney, C.S.M. and van der Plicht, J. (2013). IntCal13 and MARINE13 radiocarbon age calibration curves 0-50000 years

calBP, Radiocarbon 55(4), doi: 10.2458/azu_js_rc.55.16947

Robertson, P.K. (2012). The James K. Mitchell Lecture: Interpretation of in-situ tests – some insights, Proc. 4th Int. Conf. on Geotechnical and Geophysical Site Characterization – ISC'4, Porto de Galinhas, Brazil 1: 3-24.

Rollins, K.M. and Hollenbaugh, J.E. (2015). Liquefaction induced negative skin friction from blast-induced liquefaction tests with auger-cast piles. Procs., 6th Intl. Conf. on Earthquake Geotechnical Engineering, Christchurch, New Zealand, New Zealand Geotechnical Society, 8 p.

Rollins, K.M. and Strand, S.R. (2006). Downdrag Forces due to Liquefaction Surrounding a Pile. Proc. 8th National Conference on Earthquake Engineering, Earthquake Engineering Research Institute, 10 p.

Rollins, K.M., Lane, J.D., Nicholson, P.G. and Rollins, R.E. Liquefaction hazard assessment using controlledblasting techniques, Proc. 11th International 93 Conference on Soil Dynamics and Earthquake Engineering, 2: 630 – 637.

Servizio Geologico Sismico e dei Suoli, Regione Emilia-Romagna (2016). Banche dati territoriali, a cura di Servizio Geologico Sismico e dei Suoli, Regione Emilia-Romagna.

Tokimatsu, K. and Seed, H.B. (1987). Evaluation of Settlements in Sands Due to Earthquake Shaking, J. of Geotechnical Engineering, ASCE, 113(8): 861-878.

Tsai, P., Lee, D., Kung, G.T. and Juang, C.H. (2009). Simplified DMT-based methods for evaluating liquefaction resistance of soils, Engineering Geology ,103: 13-22.

Vannucchi, G., Crespellani, T., Facciorusso J., Ghinelli, A., Madiai C., Puliti, A., and Renzi, S. (2012). Soil liquefaction phenomena observed in recent seismic events in Emilia-Romagna Region, Italy, Ingegneria Sisimica, N. 2-3, pp. 20-30, ISSN: 03931420.

Weltje, G.J. (2002). Quantitative analysis of detrital modes: statistically rigorous confidence regions in ternary diagrams and their use in sedimentary petrology, Earth-Sci. Rev. 57, 211 – 253.

Wentz, F.J., van Ballegooy, S., Rollins, K.M. Ashford S.A. and Olsen, M.J. (2015). Large Scale Testing of Shallow Ground Improvements using Blast-Induced Liquefaction, 6ICEGE – 6th International Conference on Earthquake Geotechnical Engineering 1-4 November 2015 Christchurch, New Zealand.

Yi, F.F. (2010). Procedure to Evaluate Liquefaction-Induced Settlement Based on Shear Wave Velocity, 9th U.S. National and 10th Canadian Conference on Earthquake Engineering 9USN/10CCEE, Toronto, Canada.

Zhang, G., Robertson, P.K. and Brachman, R.W.I. (2002). Estimating liquefaction-induced ground settlements from CPT for level ground. Canadian Geotechnical Journal, 39(5): 1168-1180.